0

14pt

DEUTERIUM ABUNDANCE IN THE LOCAL ISM AND POSSIBLE SPATIAL VARIATIONS

JEFFREY L. LINSKY
JILA, University of Colorado and NIST, Boulder, CO 80309-0440 USA

Abstract. Excellent HST/GHRS spectra of interstellar hydrogen and deuterium Lyman-α absorption toward nearby stars allow us to identify systematic errors that have plagued earlier work and to measure accurate values of the D/H ratio in local interstellar gas. Analysis of 12 sightlines through the Local Interstellar Cloud leads to a mean value of $\mathrm{D/H} = (1.50 \pm 0.10) \times 10^{-5}$ with all data points lying within $\pm 1\sigma$ of the mean. Whether or not the D/H ratio has different values elsewhere in the Galaxy and beyond is a very important open question that will be one of the major objectives of the Far Ultraviolet Spectroscopic Explorer (FUSE) mission.

Key words: LISM, interstellar medium, deuterium

1. Introduction

An accurate measurement of $(\mathrm{D/H})_{\mathrm{LISM}}$, the D/H abundance ratio in the local interstellar medium (LISM), and an assessment of spatial variations of D/H in the Galaxy are required to address two critically important questions in contemporary astrophysics. First, the largest credible D/H ratio in our Galaxy will provide a lower limit to the primordial D/H ratio, $(\mathrm{D/H})_{\mathrm{prim}}$, which constrains the critical density, Ω_{B}, of baryons present in both luminous and “dark” forms. Second, $(\mathrm{D/H})_{\mathrm{LISM}}$ is the end result of an incompletely understood complex set of chemical evolution processes in the Galaxy. Comparison of the $(\mathrm{D/H})_{\mathrm{LISM}}$ ratio with D/H ratios characteristic of the protosolar nebula and in interstellar gas located elsewhere in the Galactic disk and halo will test our understanding of stellar evolution, stellar mass loss, interstellar physics, and the rate of infall and chemical composition of halo gas. Testing Galactic chemical evolution codes against both D/H and metal abundances in different environments with different histories will lead to a more detailed understanding of the evolution of our Galaxy and will test for the first time the mixing time scales for interstellar matter.

Recently, the precise value of $(\mathrm{D/H})_{\mathrm{LISM}}$ has acquired greater importance as the previously announced high value of $(\mathrm{D/H}) = 2 \times 10^{-4}$ in the absorption spectrum toward Q0014+813 is apparently spurious (Tytler *et al.* 1996). Thus $(\mathrm{D/H})_{\mathrm{LISM}}$ is likely much closer to $(\mathrm{D/H})_{\mathrm{prim}}$ than some authors had thought, and our understanding of Galactic chemical evolution will be tested by a measurement of the small difference (perhaps only a factor of 2) between $(\mathrm{D/H})_{\mathrm{prim}}$ and $(\mathrm{D/H})_{\mathrm{LISM}}$. Accurate measurements of D/H are clearly required for such tests of the chemical evolution codes and their underlying assumptions.

Lyman line absorption is generally recognized as the most reliable technique for inferring the present value of D/H in our local environment. This is a consequence of the Sun being surrounded by a cloud of warm, partially ionized gas (e.g., Lallement *et al.* 1995; Wood & Linsky 1997a) with very few molecules. At a gas temperature of about 7,000 K (Linsky *et al.* 1993), the ionization and adsorption on to grains is nearly the same for H and D. With a line separation of 81 km s^{-1}, Lyman-α absorption by H and D can be observed with high S/N in HST/GHRS spectra toward nearby stars, provided the hydrogen column density is not so large as to obliterate the D line ($N_{HI} < 10^{18.7}$ cm^{-2}). The launch of the Far Ultraviolet Spectroscopic Explorer (FUSE) in 1998 will allow us to observe the less opaque higher Lyman lines to extend this method to more distant lines of sight (LOS). Other techniques for measuring the D/H ratio, including studies of deuterated molecules in cold molecular clouds and the search for the deuterium analog of the hydrogen 21 cm line, have major difficulties, leaving the Lyman lines as the most useful D/H diagnostics.

Ferlet *et al.* (1996) reviewed D/H measurements obtained primarily with the Copernicus and IUE spectrographs. These pre-HST studies of Lyman line absorption toward both hot and cool stars left a confused picture in which the large range of permitted values of D/H for each LOS left open the possibility that D/H spatial variations of a factor of 2 or larger could be present on very short spatial scales. The flood of beautiful new GHRS spectra has changed this picture dramatically. The first clear indication of this paradigm shift was the measurement of D/H = $(1.60^{+0.14}_{-0.19}) \times 10^{-5}$ for the Capella LOS (Linsky *et al.* 1993, 1995). Since this result lies outside of the published error bars for all of the previous results for this LOS, I believe that the older results at least for the late-type stars are unreliable because of systematic errors that were not considered when these lower quality data were analyzed and thus not included in the published error bars. The GHRS spectra have allowed us to develop analysis techniques that minimize these systematic errors, leading to far more reliable values of D/H. Table I summarizes the results of these analyses of GHRS spectra.

2. Minimizing Random and Systematic Errors in the Analysis of the Lyman Lines

2.1. The effects of better quality data

GHRS echelle spectra have far higher S/N and resolution (3.6 km s^{-1}) than Copernicus (15 km s^{-1}) and IUE (25–30 km s^{-1}) spectra. Since the core

Table I
Summary of GHRS Observations of the LISM.

Star	d (pc)	l (°)	b (°)	Grating†	Clouds in LOS	D/H (10^{-5}) (in LIC)	(others)
α Cen A* [1,2]	1.3	316	–01	EA, EB	G		1.2 ± 0.7
α Cen B [2]	1.3	316	–01	EA, EB	G		1.2 ± 0.7
Sirius [1,3,4]	2.7	227	–09	EB, M	L+1	(1.65)	(1.65)
ϵ Eri [11]	3.3	196	–48	EA, EB	L	1.4 ± 0.4	
ϵ Ind [5]	3.4	336	–48	EA, EB	G/L	1.6 ± 0.4	
Procyon [6]	3.5	214	+13	EB, M	L+1	1.6 ± 0.4	
α Aql [1]	5.0	48	–09	EB	L+2		
α PsA [1]	6.7	21	–65	EB			
Vega [1]	7.5	68	+19	EB	L+2		
β Gem [11]	10.6	192	+23	EA, EB	L+1	1.4 ± 0.4	1.6 ± 0.4
β Leo [1]	12.2	251	+71	EB	L+2		
Capella* [6,7]	12.5	163	+05	EA, EB, M	L	$1.60^{+0.14}_{-0.19}$	
β Cas [8]	14	118	–03	M	L	1.6 ± 0.4	
[11]						1.7 ± 0.3	
β Cet [8]	16	111	–81	EB, M	2	2.2 ± 1.1	
β Pic [1]	16.5	258	–31	EB	L		
α Tri [11]	18	139	–31	EA, EB	L	1.6 ± 0.6	1.0 ± 0.6
λ And [5]	24	110	–15	EA	L	1.7 ± 0.5	
δ Cas [1]	27	127	–02	EB	L		
HR1099* [8]	33	185	–41	EA, EB, M	L+2	1.46 ± 0.09	
G191-B2B [9]	48	156	+07	EB, M	L+2	$1.4^{+0.1}_{-0.3}$	(1.),(1.5)
σ Gem* [11]	56	191	+23	EA, EB	L+1	1.4 ± 0.4	1.3 ± 0.4
HZ 43 [12]	63	054	+84	EA, EB	NGP		(1.6)
31 Com [8]	80	115	+89	EB, M	NGP		1.5 ± 0.4
[11]							2.0 ± 0.4
ϵ CMa [10]	187	240	–11	EB, M	L+5	(1.65)	

Quantities in parenthesis are assumed D/H values that lead to good profile fits.
* These stars were observed twice. Capella, HR 1099 and σ Gem were observed near opposite quadratures.
† Gratings: EA = Echelle-A, EB = Echelle-B, M = G140M or G160M.
References: [1] Lallement *et al.* (1995), [2] Linsky & Wood (1996), [3] Lallement *et al.* (1994), [4] Bertin *et al.* (1995), [5] Wood *et al.* (1996), [6] Linsky *et al.* (1995), [7] Linsky *et al.* (1993), [8] Piskunov *et al.* (1997), [9] Lemoine *et al.* (1996), [10] Gry *et al.* (1995), [11] Dring *et al.* (1997), [12] Landsman *et al.* (1996).

of the Lyman-α line is very saturated (optical depths of 10^5 – 10^6) and is located on the flat part of the curve of growth, high S/N and spectral resolution are critical for inferring H column densities from the steep outer edges of the core absorption profile. Even with the best available GHRS spectra, however, the H column densities are usually more uncertain than the

D column densities. Accurate fits to the outer edges of the core absorption alone may explain much of the previous scatter in the D/H values.

2.2. Systematic errors introduced by complex velocity structure and uncertain hydrogen predictors

Another critical issue is the presence of absorption components at many velocities in a stellar spectrum. For example, ultra-high resolution spectra of the Na I and Ca II resonance lines typically show many closely spaced narrow velocity components even for short LOS (e.g., Welty *et al.* 1996). Since thermal broadening is much larger in the low mass H and D lines than in the metal lines, it is difficult to isolate the absorption due to individual velocity components in the H and D lines. One can include these velocity components in the analysis of the H and D lines, but the relative column densities observed in the metal lines may not be good predictors of the relative column densities in the H and D lines. It is commonly assumed that N I and O I are good predictors of H I and D I column densities because all four species have nearly the same ionization potentials and thus should have the same ionization equilibria. However, Vidal-Madjar (these proceedings) showed that for the three velocity components along the LOS to the hot white dwarf G191-B2B, the D/N column density ratios differ by a factor of 3 and the D/O column density ratios differ by a factor of 10. Since there is no apparent explanation for these large discrepancies, one must conclude that even N I and O I are not infallible predictors of H column densities. Thus it is difficult to infer D/H for individual velocity components along a complex LOS, and the inferred mean value of D/H along a LOS could be biased by saturation.

2.3. Systematic errors introduced by hydrogen walls

Velocity components with column densities orders of magnitude smaller than the main interstellar absorption component pose an especially difficult problem, since these components are not detectable in metal lines, but they could be optically thick in the H Lyman-α line. Linsky and Wood's (1996) analysis of the very short (1.3 pc) LOS to α Cen A and α Cen B shows that by not including such velocity components when they are present the inferred H column densities can be a factor of 2 too large and the D/H ratios can thus be a factor of 2 too small.

The upper panel of Figure 1 shows the observed Lyman-α profile toward α Cen B and Linsky & Wood's best fit model in which the velocity and temperature of the interstellar H I are constrained to be the same as the values obtained by fitting the D I, Mg II, and Fe II lines. Clearly there is missing opacity near zero observed flux on the red side of the interstellar

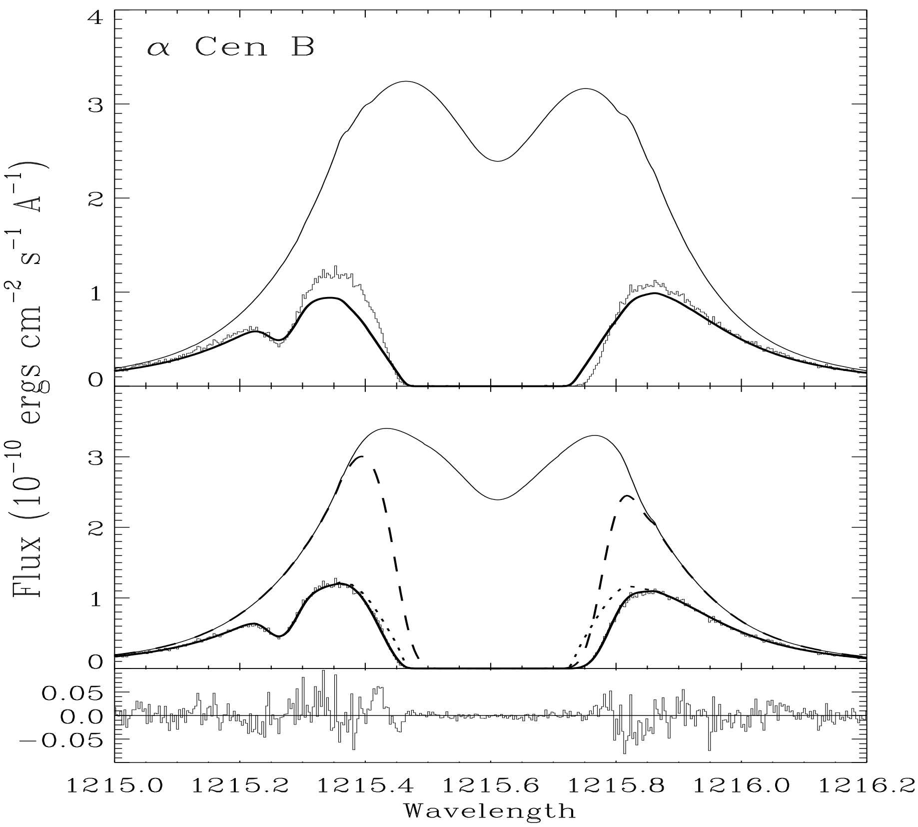

Figure 1. Upper panel: comparison of the observed Echelle-A spectrum (noisy line) of α Cen B with the assumed intrinsic stellar spectrum (smooth thin line) and the best constrained one-component model fit (thick solid line). Middle panel: best two-component model with the absorption due to the ISM component only (dotted line), absorption due to the H wall component only (dashed line), and the total absorption (thick solid line). Lower panel: residuals between the observed profile and the two-component fit (from Linsky & Wood 1996).

absorption, indicating the need to include additional absorption by gas that (i) is redshifted compared to the interstellar flow velocity of 18.0 km s^{-1}, (ii) is hotter than the interstellar gas (required to fit the gentler slope of the red side of the absorption compared to the blue side), and (iii) has a relatively low column density (the additional absorption has no Voigt wings). Because there is missing opacity at zero flux, no sensible change in the assumed intrinsic stellar profile can explain the discrepancy. The middle panel of Figure 1 shows their least-squares fit to the observed profile by a two-component model. The first component of this model has the same interstellar velocity and broadening parameters as those derived from the

D I, Mg II, and Fe II lines, but a smaller hydrogen column because the second component will explain the deep absorption on the red side of the interstellar absorption feature. The gas in the second component turns out to be hot ($T = 29,000 \pm 5,000$ K), has a low column density ($\log N_{\rm H\ I} = 14.74 \pm 0.24$), and is redshifted by 2–4 km s^{-1} relative to the main component of the interstellar gas. Given the highly saturated nature of the main component, the inclusion of this second component, even though it has only 1/1000 the H column density of the first component, lowers the hydrogen column of the first component by a factor of 2 and thereby raises the inferred D/H ratio from $\approx 6 \times 10^{-6}$ to $(1.2 \pm 0.7) \times 10^{-5}$. The uncertainty in D/H is large because there are many parameters to be determined.

When Linsky and Wood derived these results they were unaware of the location of the second absorption component of H I along the LOS to α Cen. The location became clear later at the 1995 July 12-13 meeting of the IUGG in Boulder, Colorado, where Baranov, Zank, and Williams presented their calculations of the interaction between the solar wind and the incoming interstellar flow. Their models (Baranov *et al.* 1995a, 1995b; Pauls *et al.* 1995), which include charge exchange between the outflowing solar wind protons and the inflowing H I atoms, show that on both sides of the heliopause there is a region of decelerated, hot hydrogen with higher density than in the LIC (see Fig. 2). This H I pileup region, which is located about 200 AU in the upstream direction (depending on the proton density in the LIC), has been called the "hydrogen wall." Because the computed column density, temperature, and flow velocity of H I in the hydrogen wall agree with the parameters derived independently for the second component toward α Cen, Linsky and Wood (1996) concluded that the second component originates in the wall around the heliosphere. Before this time the hydrogen wall was an interesting theoretical concept with no observational confirmation, although Lyman-α backscattering observations (e.g., Quémerais *et al.* 1995) indicated that $n_{\rm H\ I}$ increases outward toward the heliopause.

Do hydrogen walls exist around other stars? A stellar hydrogen wall would be seen as a second absorption component shifted to shorter wavelengths compared to the interstellar gas flowing toward the star, because in order to detect the stellar wall it would have to be viewed from the upwind direction. Wood, Alexander, & Linsky (1996) found that a one-component model for the interstellar absorption toward ϵ Ind could not explain the absorption on the blue side of the interstellar Lyman-α line. They concluded that a second component blueshifted by 18 ± 6 km s^{-1} with respect to the interstellar flow was needed with $\log N_{\rm H\ I} = 14.2 \pm 0.2$ and $T = 100,000 \pm 20,000$ K. The high temperature and large blueshift are consistent with the higher inflow velocity of 64.0 km s^{-1} toward this rapidly moving star. They also found evidence for a hydrogen wall around λ And with a smaller blueshift and temperature. Dring *et al.* (1997) showed that a H wall is also present

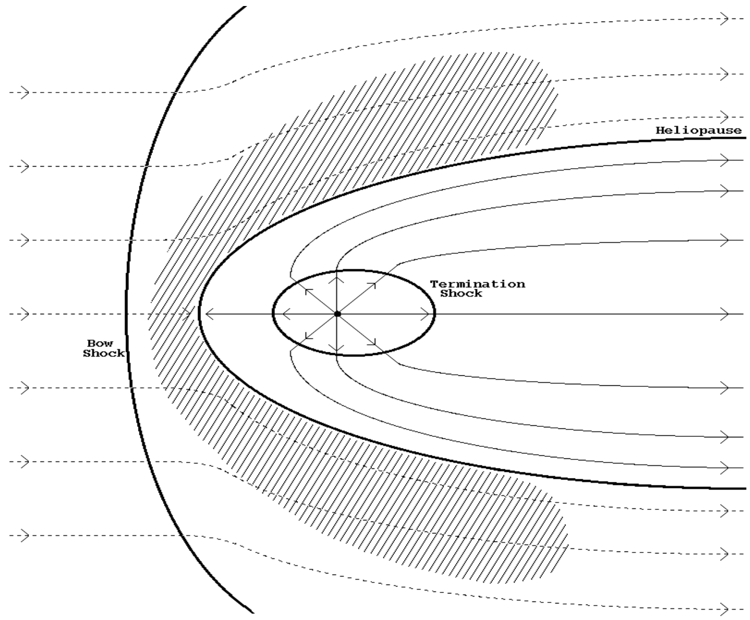

Figure 2. A schematic picture of the heliosphere showing the bow shock (where the incoming interstellar gas flow becomes subsonic), the termination shock (where the solar wind becomes subsonic), the heliopause surface dividing the two plasma flows, and the general location of the hydrogen wall (shaded region) where the inflowing neutral hydrogen is decelerated, compressed and heated by charge exchange reactions with solar wind protons. The hydrogen wall actually extends into the heliopause toward the termination shock.

around ϵ Eri, and Wood & Linsky (1997b) found evidence for hydrogen walls around the high velocity stars 61 Cyg A and 40 Eri A. Thus the inclusion of solar and stellar hydrogen wall absorption when the viewing angles are appropriate is required for obtaining accurate D/H values.

2.4. Systematic errors introduced by the unknown emission line profile

Another source of systematic errors is the unknown stellar Lyman-α emission line which serves as the "continuum" against which one measures interstellar absorption. One method for minimizing this problem is to analyze spectroscopic binary systems observed at opposite quadratures (when the orbital radial velocities are a maximum) so that the combined stellar emission line

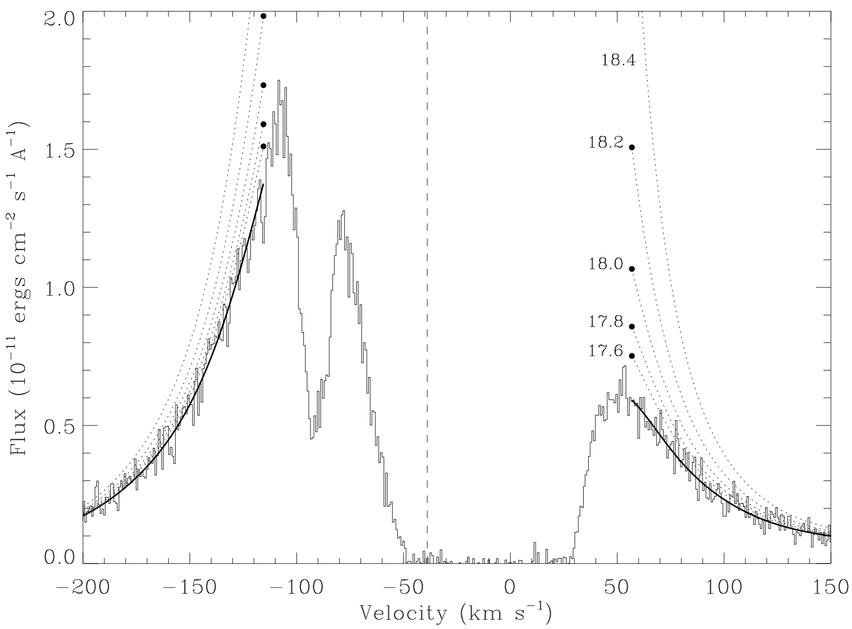

Figure 3. Reconstructions of the wings of the Lyman-α line profile of ϵ Ind assuming different values of $\log N_{\mathrm{H\ I}}$ (numbers next to the dotted lines). The thick solid lines are polynomial fits to the wings of the observed Lyman-α profile. The dotted lines are estimates of the intrinsic Lyman-α line wings for different assumed values of $\log N_{\mathrm{H\ I}}$. The selected best value for $\log N_{\mathrm{H\ I}}$ is that which produces a stellar emission line centered on the stellar radial velocity (dashed line) (from Wood *et al.* 1996).

profile has a different shape in the two observations, whereas the interstellar absorption is unchanged. The additional information provided by the two observations allows one to infer the intrinsic stellar emission line profiles and the interstellar absorption nearly independent of each other. Linsky *et al.* (1995) and Piskunov *et al.* (1997) have used this approach to analyze the LOS toward Capella and HR 1099, and Dring *et al.* (1997) have used a similar approach to study the LOS toward σ Gem.

High radial velocity stars provide an opportunity for deriving $N_{\mathrm{H\ I}}$ more accurately from the optically thin line wings than from the saturated core. For the star ϵ Ind, Wood *et al.* (1996) inferred the interstellar Lyman-α wing absorption (see Fig. 3) by reconstructing the stellar Lyman-α emission line wings assuming only that they are symmetric about the stellar radial velocity (-38.9 km s^{-1}).

3. Kinematic and Physical Properties of the LISM

Lallement and Bertin (1992) proposed that the Sun lies inside a cloud, which they called the Local Interstellar Cloud (LIC), because the LOS velocities toward 6 nearby stars observed in ground-based Ca II spectra and the velocity of interstellar He I flowing into the solar system are consistent with a single flow vector. GHRS spectra of the Mg II and Fe II resonance lines (2796, 2803, and 2600 Å) formed in the LOS toward other nearby stars (Lallement *et al.* 1995) confirmed this picture with the flow vector magnitude 26 ± 1 km s^{-1} directed from Galactic coordinates $l = 186° \pm 3°$ and $b = -16° \pm 3°$ in the heliocentric rest frame. In the local standard of rest (defined by the motion of nearby stars), the LIC flow is from Galactic coordinates $l = 331.9°$ and $b = +4.6°$. The direction of this flow suggests that it originates from the expansion of a large superbubble created by supernovae and stellar winds from the Scorpius-Centaurus OB Association (Crutcher 1982; Frisch 1995).

GHRS spectra are confirming that the kinematical structure of the LISM is indeed very complex. Most lines of sight show at least one velocity component in addition to the LIC, even for stars as close as Sirius (2.7 pc) and Procyon (3.5 pc), indicating that additional clouds lie outside of the LIC at short distances. Table I lists the specific clouds now identified on the LOS toward the stars observed with the GHRS, where L refers to the LIC. In the Galactic Center direction the Sun lies close to the edge of the G cloud as the α Cen stars show interstellar absorption only at the velocity of this cloud. The Sun also likely lies very close to the edge of the LIC toward the North Galactic Pole as 31 Comae (Piskunov *et al.* 1997) shows only one velocity component that is inconsistent with the LIC vector.

The temperature and nonthermal broadening of interstellar gas can be measured by comparing line widths of low mass elements (H and D) and high mass elements (e.g., Mg and Fe). For the LOS to Capella, Linsky *et al.* (1995) derived $T = 7000 \pm 500 \pm 400$ K and $\xi = 1.6 \pm 0.4 \pm 0.2$ km s^{-1}, where the second uncertainty refers to the likely systematic errors due primarily to the uncertain intrinsic stellar emission lines. They also found $T = 6900 \pm 80 \pm 300$ K and $\xi = 1.21 \pm 0.27$ for the Procyon LOS. Temperatures and turbulent velocities measured for other LOS through the LIC are consistent with these values. For example, Lallement *et al.* (1994) found that $T = 7600 \pm 3000$ K and $\xi = 1.4^{+0.6}_{-1.4}$ km s^{-1} for the LIC component toward Sirius, and Gry *et al.* (1995) found that $T = 7200 \pm 2000$ K and $\xi = 2.0 \pm 0.3$ km s^{-1} for the LIC component toward ϵ CMa. Recent analyses (Piskunov *et al.* 1997) of the LIC components toward HR 1099, 31 Com, β Cet, and β Cas yield similar results, and *in situ* measurements of the LISM H I and He I atoms flowing through the heliosphere (cf. Lallement *et al.* 1994) yield consistent values for the temperature. I therefore conclude that $T \approx 7000$ K and $\xi \approx 1.2$ km s^{-1} in the LIC.

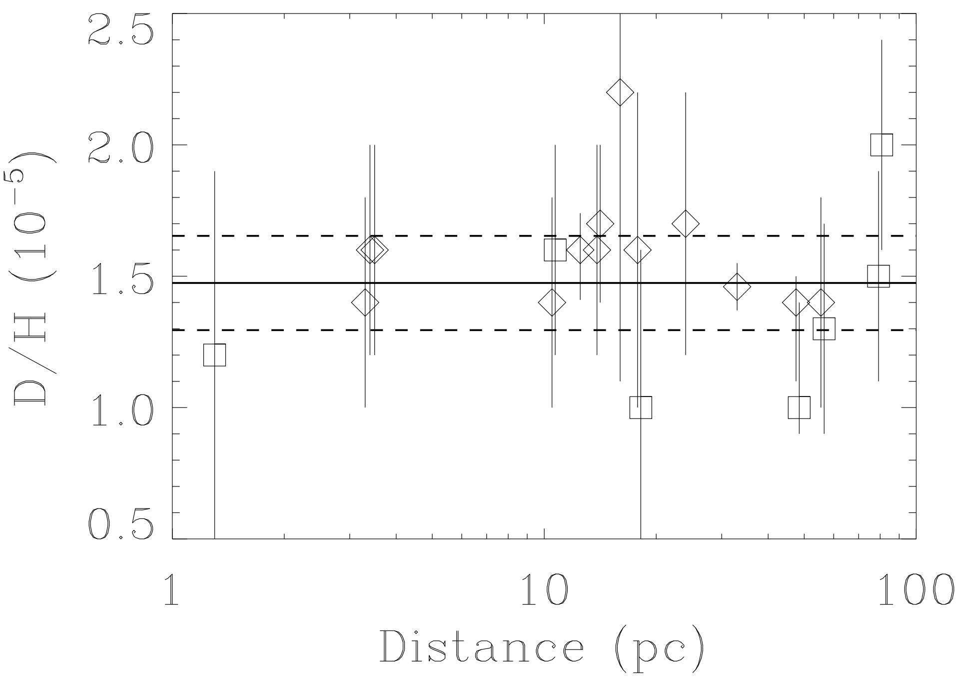

Figure 4. D/H ratios for interstellar gas toward all nearby stars observed with the GHRS. Diamond symbols are for gas in the LIC and square symbols are for other warm clouds. The solid and dashed horizontal lines represent the mean value of D/H and the $\pm 1\sigma$ error of the mean for all data points.

Other clouds have different parameters. The G cloud, for example, is cooler with $T = 5400 \pm 500$ K and $\xi = 1.20 \pm 0.25$ km s^{-1} along the LOS to α Cen. Component 2 toward ϵ CMa is also cooler with $T = 3600 \pm 1500$ K and $\xi = 1.85 \pm 0.3$ km s^{-1} (Gry *et al.* 1995). Hotter gas is inferred for several clouds toward ϵ CMa and for some of the gas toward Sirius (Bertin *et al.* 1995).

4. A Summary of What is Now Known about D/H in the LISM

Table I lists all of the published D/H values derived for different clouds along the LOS toward nearby stars with GHRS observations. Quantities in parenthesis are assumed rather than derived and are not included in the subsequent analysis. Figure 4 shows the derived D/H ratios for 12 stars with interstellar radial velocities indicating that their LOS pass through the

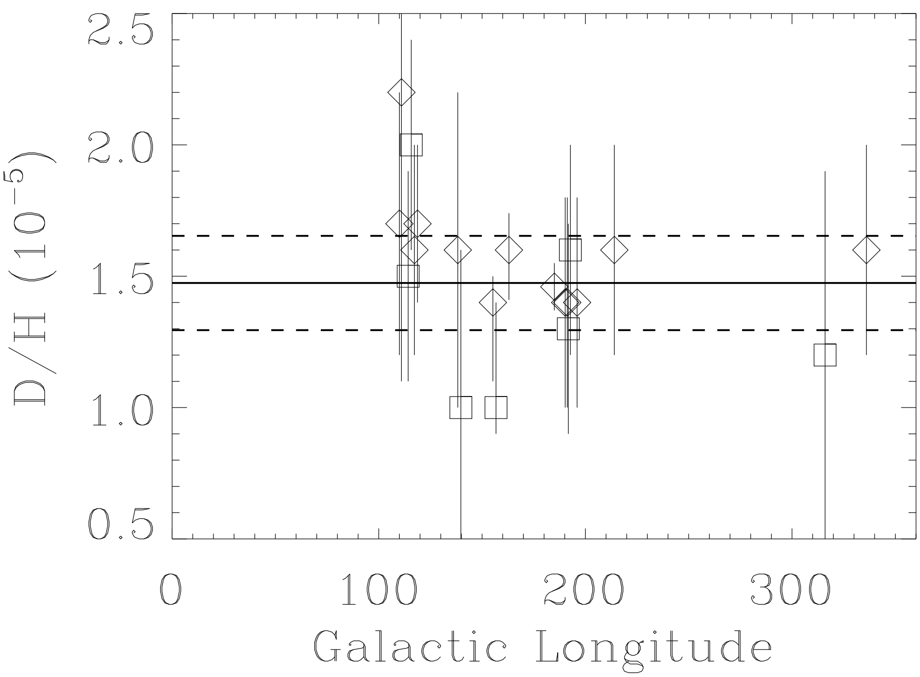

Figure 5. Same as Figure 4, except that the D/H ratios are plotted with respect to Galactic longitude.

Local Interstellar Cloud (LIC) and 7 stars with LOS that pass through other nearby warm clouds. The mean value for the LIC is (D/H) $= (1.50 \pm 0.10) \times 10^{-5}$ and the $\pm 1\sigma$ error bars for all 12 data points are consistent with the mean value. The horizontal and dashed lines in Figure 4 show the mean relation for all data points, (D/H) $= (1.47 \pm 0.18) \times 10^{-5}$. This figure shows that there is no trend in the D/H ratios with distance. Figure 5, in which the same data are plotted with respect to Galactic longitude, shows that there is no trend with Galactic longitude either.

The LIC data lead me to conclude that the value of D/H in the tiny region of the Galaxy occupied by the LIC is constant and reasonably well known, but we are just beginning to sample more distant lines of sight which may show different D/H ratios. The data for the other clouds are more scattered with (D/H) $= (1.28 \pm 0.36) \times 10^{-5}$. Whether or not this scatter represents measurement errors or indicates real D/H differences between the LIC and the other clouds can only be answered with more high quality observations obtained with FUSE and STIS. FUSE will observe the less opaque high Lyman lines and thus permit us to study D/H further out in the Galactic disk, in the Galactic halo, and along some LOS toward active galactic nuclei. These spectra will be a challenge to analyze compared to the GHRS spectra because the resolution (10–12 km s^{-1}) and S/N will be lower and the LOS toward the more distant targets will be complex. Nevertheless, we look forward to analyzing the FUSE data after the launch of the satellite scheduled for October 1998.

This work is supported by NASA through grant S-56460-D. I thank Dr. Brian Wood for the many discussions and collaborations upon which this review is based. I also thank ISSI for its hospitality and support.

References

Baranov, V. B., & Malama, Y. G.: 1995a, *JGR*, **98**, 15157.
Baranov, V. B., & Malama, Y. G.: 1995b, *JGR*, **100**, A8, 14755.
Bertin, P., Vidal-Madjar, A., Lallement, R., Ferlet, R., & Lemoine, M.: 1995, *A&A*, **302**, 889.
Crutcher, R.M.: 1982, *ApJ*, **254**, 82.
Dring, A.R., Linsky, J., Murthy, J., Henry, R.C., Moos, W., Vidal-Madjar, A., Audouze, J., & Landsman, W.: 1997, *Ap.J.*, in press.
Ferlet, R. *et al.* in *Science with the HST-II*, ed. B. Benvenuti *et al.* (Space Telescope Science Institute, Baltimore, 1996), p. 450.
Frisch, P. C.: 1995, *Science*, **265**, 1423.
Gry, C., Lemonon, L., Vidal-Madjar, A., Lemoine, M., & Ferlet, R, 1995, *A&A*, **302**, 497.
Lallement, R., & Bertin, P.: 1992, *A&A*, **266**, 479.
Lallement, R., Bertin, P., Ferlet, R., Vidal-Madjar, A., & Bertaux, J. L.: 1994, *A&A*, **286**, 898.
Lallement, R., Ferlet, R., Lagrange, A. M., Lemoine, M., & Vidal-Madjar, A.: 1995, *A&A*, **304**, 461.
Landsman, W., Sofia, U.J., & Bergeron, P.: 1996, in *Science with the HST-II*, ed. B. Benvenuti *et al.* (Space Telescope Science Institute, Baltimore), p. 454.
Lemoine, M., Vidal-Madjar, A., Bertin, P., Ferlet, R., Gry, C., and Lallement, R.: 1996, *A&A*, **308**, 601.
Linsky, J. L., Brown, A., Gayley, K., Diplas, A., Savage, B. D., Ayres, T. R., Landsman, W., Shore, S. N., & Heap, S. R.: 1993, *Ap.J.*, **402**, 694.
Linsky, J. L., Diplas, A., Wood, B. E., Brown, A., Ayres, T. R., & Savage, B. D.: 1995, *Ap.J.*, **451**, 335.
Linsky, J. L. & Wood, B. E.: 1996, *Ap.J.*, **463**, 254.
Pauls, H. L., Zank, G. P., & Williams, L. L.: 1995, *JGR*, **100**, 21595.
Piskunov, N., Wood, B., Linsky, J. L., Dempsey, R. C., & Ayres, T. R.: 1997, *Ap.J.*, **474**, 315.
Quémerais, E., Sandel, B. R., Lallement, R., & Bertaux, J.-L.: 1995, *A&A*, **299**, 249.
Tytler, D., Burles, S. & Kirkman, D.: 1997, *Ap.J.*, in press.
Welty, D. *et al.*, *Ap.J. Suppl.* **106**, 533 (1996).
Wood, B.E. & Linsky, J.L.: 1997a, *Ap.J*, **474**, L39.
Wood, B.E. & Linsky, J.L.: 1997b, *Ap.J*, in press.
Wood, B. E., Alexander, W. R., & Linsky, J. L.: 1996, *Ap.J.*, **470**, 1157.